Influence of phase transition and photoisomerization on interfacial rheology

Kang Sub Yim and Gerald G. Fuller
Department of Chemical Engineering, Stanford University, Stanford, California 94305
(Received 31 January 2002; revised manuscript received 5 December 2002; published 11 April 2003)

This paper presents the shear responses and interfacial rheology of photosensitive monolayers. Langmuir films of a fatty acid containing an azobenzene moiety that can undergo *trans-cis* photoisomerization have been investigated for their structural and dynamical properties. The *cis* conformation produces a structureless, Newtonian film that cannot be oriented by surface flows. Transforming the molecule to the *trans* configuration produces a well-packed film that responds to flow with an anisotropic and non-Newtonian character. The *trans* state supports two separate phases, a low-pressure phase where the azobenzene group is free to rotate, and a high-pressure phase where this moiety is frozen in place.

DOI: 10.1103/PhysRevE.67.041601 PACS number(s): 68.18.−g

1. INTRODUCTION

Photosensitive materials are able to respond to light by altering their structure and conformation and these changes are accompanied by variations of their physical properties. Photochromic phenomena of photosensitive materials have attracted attention due to the possibility of exploiting these effects in photomodulated sensors and devices. This is mainly due to the advantages of sensitivity and stability compared with properties derived from conventional, mechanical induced process.

The photoinduced *trans-cis* isomerization of azobenzene-containing molecules is a well-known photochromic phenomenon that has been extensively studied for various electro-optical applications [1–3]. Some of the azobenzene-containing amphiphiles are known to have liquid crystalline phases in very thin films [4,5]. The orientation and packing of the molecules within the films affect their optical characteristics, which is important in the eventual design of optoelectric devices.

A moiety that is capable of strong photoisomerization transitions is the azobenzene group, which undergoes geometric changes upon illumination by UV on visible light. The *trans* planar isomer, which has a rod-shaped configuration, is transformed to the bent-shaped *cis* conformations in which the —N═N— group is in a plane perpendicular to the phenylene groups. The isomerization involves a decrease of the distance between the *para* carbon atoms in azobenzene from about 9.0 Å in the *trans* form to 5.5 Å in the *cis* form. Likewise, *trans*-azobenzene has almost no dipole moment (0–0.5 D), while the dipole moment of the *cis* compound is 3.0–3.5 D [6]. This large conformational and physicochemical change induced by isomerization is reversible and makes azobenzene a candidate for photoelectronic applications.

Recently, a number of investigations have considered Langmuir-Blodgett (LB) films consisting of organized molecular assemblies in the form of ultrathin layers. The molecular structure and orientation in LB films inherently depend on the state of molecular configuration in the precursor, spread monolayer at the air/water interface. In addition, they are also influenced by the coupling of the film microstructure to surface flows associated with the deposition process. For this reason, it is important to understand the interplay between the molecular structure of fluid interfaces (e.g., the role of phase transitions and isomerization in this paper) and surface rheology.

This study combines classical measurements used to establish the thermodynamic state of Langmuir monolayers (e.g., surface pressure–molecular area isotherms) with methods devised to reveal the orientation dynamics of these systems under flow (e.g., interfacial stress rheometry, UV dichroism, and flow–Brewster angle microscopy). Dimensionality has a profound influence on thermodynamics, and Langmuir monolayers are known to have rich phase diagrams. Amphiphiles such as fatty acids, alcohols, and phospholipids [7] have been extensively studied. These systems show complicated but well-ordered phase diagrams and transitions at the air/water interface. The structure of the corresponding phases has been established using x-ray diffraction and Brewster angle microscopy (BAM). The dynamics of Langmuir monolayers also reveal the strong influence of dimensionality. These systems display a variety of nonlinear surface rheological behaviors that include complex surface moduli, shear thinning surface viscosities, and nematiclike flow responses [8–10]. However, the relationship between thermodynamic structures and their rheological responses has rarely been reported for two-dimensional systems.

This paper reports measurements on an azobenzene-containing amphiphile, 4-octyl-4′-(3-carboxytrimethyleneoxy) azobenzene (C_8AzC_3). This fatty acid derivative has the useful properties of undergoing thermodynamic phase transitions like simple fatty acids as well as *trans*-to-*cis* photoisomerization upon the application of UV-visible light. In this manner, this molecule offers the possibility of examining the ability of molecules to efficiently pack at the interface and the effects on both thermodynamics and orientational dynamics. The presence of the azobenzene group with its strong, polarization-dependent absorption in the ultraviolet allows UV dichroism measurements to be applied to obtain sensitive determinations of flow-induced orientation. For these reasons C_8AzC_3 is a good model material for identifying the relationship between the thermodynamic phase structure and the rheological orientational dynamics at the air/water interface.

The degree of molecular order in two-dimensional monolayers can be determined from the anisotropy in the absorption of light by the layer, which results in a linear dichroism $\Delta n'' = n_1'' - n_2''$ in the sample, where n_1'' and n_2'' are the prin-

cipal values of the imaginary part of the refractive index. We have previously applied visible light dichroism to this problem but it is found that UV light has a higher sensitivity in absorption than visible light for studying liquid crystalline molecules including C_8AzC_3 [9]. In our experiments, the dichroism is measured dynamically by rapidly modulating the polarization of the UV light incident on the sample [11] and the measurements are acquired *in situ* on flowing monolayers.

Here, we study the phase diagram and domain structure of the azobenzene derivative fatty acid C_8AzC_3 by conventional isotherm measurements and by BAM. The coupling of the phase structure and orientational dynamics is then examined using UV dichroism under extensional flow and the measurement of interfacial rheology. In addition, the effect of *trans-cis* photoisomerization on molecular anisotropy will be discussed.

II. MATERIALS AND METHODS

The azobenzene-containing fatty acid 4-octyl-4′-(3-carboxytrimethyleneoxy) azobenzene (C_8AzC_3), with the molecular structure

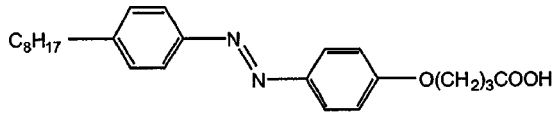

C_8AzC_3

was obtained from Dojindo Laboratories and dissolved in chloroform to form the spreading solution. Docosanoic acid (C_{22}) was purchased from Sigma. Two Langmuir minitroughs made of Teflon measuring $25.0\times7.5\ cm^2$ and a $35.0\times7.5\ cm^2$, respectively, were used for all measurements (KSV Instruments, Finland). The surface pressure was monitored using a Wilhelmy balance. All experiments were performed at $22\pm0.1\,°C$ unless stated otherwise.

The *trans-cis* photoisomerization of C_8AzC_3 is induced by alternatively irradiating the film with a UV lamp of 365 nm (UVLMS-38, UVP) and white light. The UV absorption spectrum in chloroform solution was recorded using a diode array spectrophotometer (HP 8452A).

The rollers of the four-roll mill were positioned to generate an extensional flow for studying flow-induced molecular orientation (Fig. 1). The diameter of the rollers was 1.98 cm and the distance between adjacent rollers was 3.18 cm. This ratio of roller diameter to roller spacing, 0.625, provides the closest approximation to homogeneous extension for bulk flows [12]. The compression and extension axes in this flow can be interchanged by simply reversing the direction of roller rotation. All measurements were performed in the stagnation region located at the geometric center of the rollers, where material has a long residence time.

Brewster angle microscopy was utilized to visualize the morphology of the monolayer mixtures. *P*-polarized light from a 10 mW argon laser was used as light source. The reflected beam was sent through an analyzer to enhance contrast and recorded with a charge-coupled device camera.

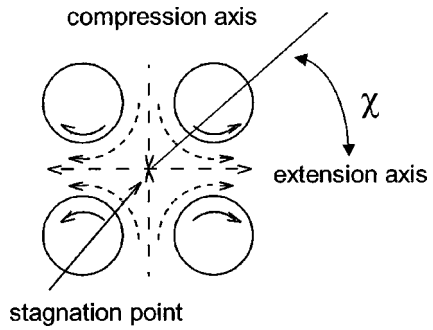

FIG. 1. Top view of the four-roll mill to produce extensional flow. The direction of roller rotation and the resulting flow field are shown. A stagnation point of the flow field exists at the center of the device. For the roller rotation in the figure, the compression axis is the vertical line of symmetry as the extension axis is the horizontal line of symmetry.

A description and analysis of the optical train for the dichroism measurements have been discussed previously [9]. In this study, the UV light of 275 nm generated using an argon laser (Spectra-Physics 2085-20RS) and transmitted through the monolayer is measured using a photomultiplier tube. The dichroism is recovered as an anisotropy parameter $\delta''=(2\pi\Delta n''d)/\lambda$, where d is the thickness of the monolayer and λ is the wavelength of the incident light.

An interfacial stress rheometer was recently constructed to study the rheology of Langmuir monolayers [13]. A magnetized rod oscillates at the air/water interface by applying a sinusoidal magnetic field gradient. The dynamic surface moduli $G_s^*(\omega)$ can be obtained by measuring the amplitude and phase of the resulting rod motion relative to the applied force. Similarly, the dynamic surface viscosity $\mu_s^*(\omega)$ is easily derived from the dynamic moduli from the simple rheological equation

$$\mu_s^*(\omega)\equiv\mu_s'(\omega)-i\mu_s''(\omega)=\frac{G_s^*(\omega)}{i\omega}=\frac{G_s''(\omega)}{\omega}-i\frac{G_s'(\omega)}{\omega},$$

where ω is the frequency. G_s', μ_s' and G_s'', μ_s'' represent the real and imaginary parts, respectively.

III. RESULTS AND DISCUSSION

A. Absorption spectrum of azobenzene-containing fatty acid C_8AzC_3

Figure 2 shows the absorption spectral changes of C_8AzC_3 in chloroform solution. The maximum absorption peak centered at 350 nm is attributed to the π-π^* transition along the long axis of the *trans* isomer [14] [Fig. 2(a)]. Irradiation with UV light causes a gradual decrease of the π-π^* transition band (350 nm), while the n-π^* transition band (444 nm) increases during UV irradiation [Fig. 2(b)], indicating the occurrence of *trans*-to-*cis* photoisomerization. The *cis* isomer thus produced can be reconverted to the *trans* isomer using visible illumination, which results in a recovery of the spectral features of the *trans* isomer.

Another absorption maximum of a shorter wavelength is found at 250 nm irrespective of the photoisomerization,

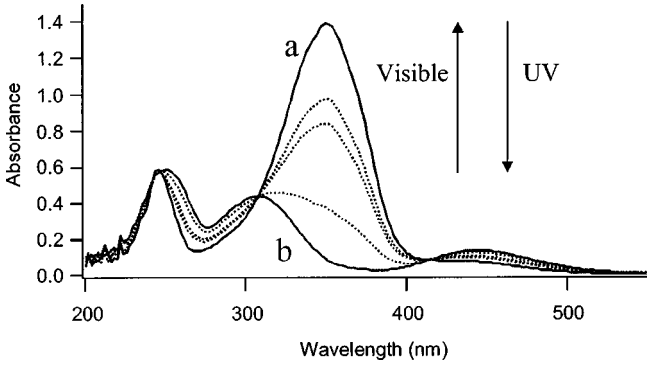

FIG. 2. Absorption spectra of C_8AzC_3 in chloroform solution in response to UV and visible irradiation: (a) *trans* isomer; (b) *cis* isomer; dotted lines are intermediate states obtained by UV or visible illumination.

which has been identified as the electronic transition moment parallel to the short axis of azobenzene [14]. It has been reported that a redshift of 10–25 nm of the maximum band occurs for thin films compared to the chloroform solution due to the excitonic interactions between the chromophores and aggregation in the film environment [15–17]. Therefore, this redshifted absorption maximum on monolayers almost corresponds to the wavelength of the argon laser (275 nm), which allows us to measure UV dichroism for the study of orientational dynamics.

B. Isotherms and phase transition

Figure 3 shows surface pressure/surface area isotherms for monolayers in both the *trans* and *cis* configurations. To produce the *trans* form, the monolayers were spread in the absence of light and the *cis* form was produced by irradiating the spread layers with ultraviolet radiation. The two molecular configurations produce qualitatively different isotherms, with the *trans* form being much less compressible and exhibiting a first order phase transition at a surface pressure of 13.4 mN/m.

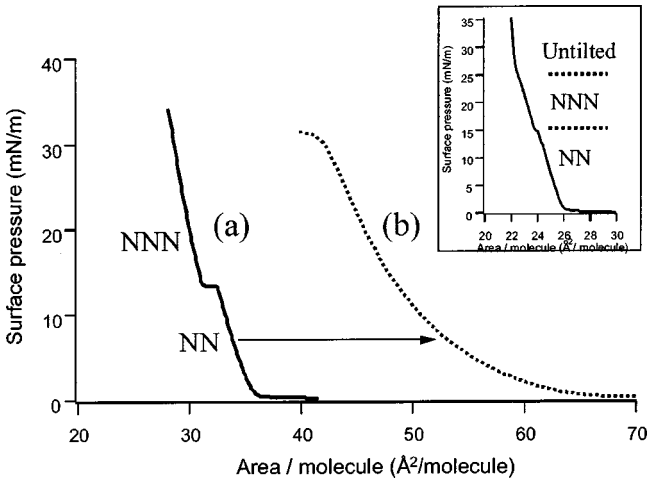

FIG. 3. Surface pressure–area isotherms for C_8AzC_3 monolayers at 22 °C. (a) *trans* isomer; (b) *cis* isomer after 10 min of 365 nm irradiation (1 mW/cm^2). Inset is an isotherm of docosanoic acid at 15 °C.

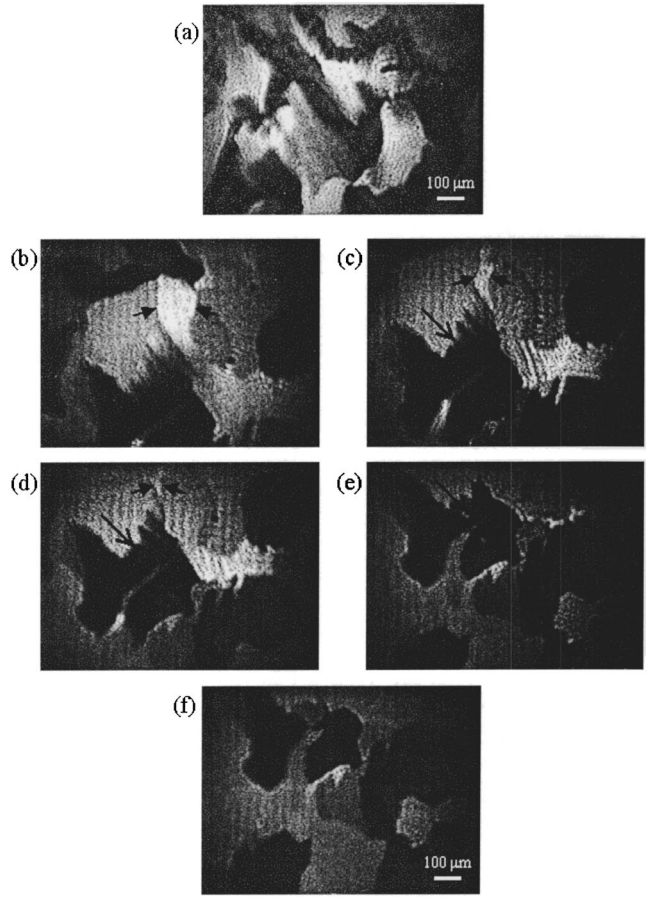

FIG. 4. A series of BAM images in the *trans* phase. (a) NN phase at 13 mN/m of the *trans* isomer; (b)–(e) the intermediate phases during the transition from NN to NNN phase. Each image is taken at a time interval of 3 s. (f) NNN phase after transition. Arrows represent the domain growth during transition.

It has been suggested from x-ray diffraction studies on C_8AzC_3 monolayers that this first order transition corresponds to the transition from a nearest neighbor (NN) to a next-nearest neighbor (NNN) tilt [18]. Compared with first order phase transitions studied on classic fatty acids [for example, docosanoic acid (C_{22}), which produces the isotherm shown in the inset of Fig. 3], C_8AzC_3 is distinguished in two ways: the coexistence region is much larger, and the tilt angle of this molecule is insensitive to surface pressure within each phase. It is believed that the strength of the phase transition is due to van der Waals interactions between molecules, and that the constant tilt angle is due to the fact that molecules are prevented from sliding against each other, which indicates that azobenzene derivatives have stronger interactions and more complicated structures than aliphatic fatty acids [18].

The limiting areas of the NN and NNN tilted phases were found to be 35.7 and 32.9 Å^2/molecule, respectively, which are larger than the cross-sectional area perpendicular to the long axis of the azobenzene group (25.2 Å^2/molecule) [19]. This is additional evidence that C_8AzC_3 has a tilted orientation at the air/water interface. The surface area A_t and the cross-sectional area A_c normal to the molecular axis are re-

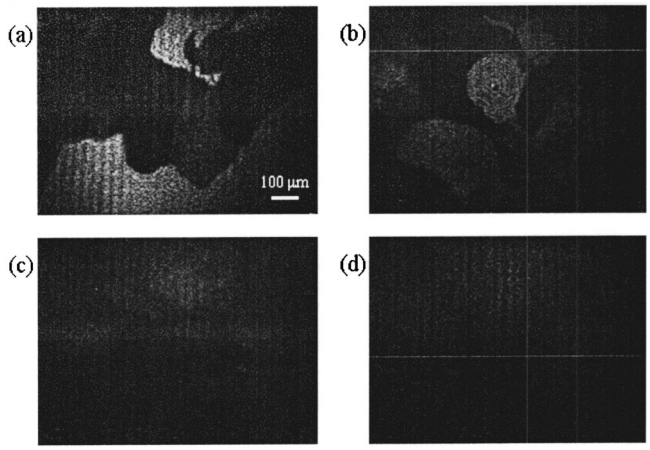

FIG. 5. Morphological changes of C_8AzC_3 monolayer during *trans*-to-*cis* photoisomerization induced by unpolarized UV of 365 nm (1 mW/cm^2). Images were taken at 15 mN/m before irradiation (a), and after irradiation for 2 (b), 3 (c), and 3.5 s (d).

lated to the tilt angle θ by simple geometry according to $A_t = A_c/\cos\theta$. From this equation, the tilt angle θ can be estimated. Using the limiting areas in the isotherm, tilt angles of 45° and 40° were calculated for the NN and NNN phases, respectively, which are close to those obtained in previous studies [18,20].

The *cis* isomer produces a much more compressible layer and lacks any evidence of a phase transition. In addition, the surface area per molecule is markedly higher for the *cis* configuration, which reflects the more efficient packing possible with the *trans* state. The molecules clearly have different arrangements and interactions within the monolayer depending on the conformation of the azobenzene moieties. The existence of higher collapse pressure for the *trans* isomer (38 mN/m) compared to the *cis* isomer (30.5 mN/m) suggests that intermolecular interactions are stronger in *trans* monolayers.

The morphologies of C_8AzC_3 monolayers are shown in Fig. 4 during the NN to NNN transition of the *trans* isomer by BAM. Both the NN [Fig. 4(a)] and NNN [Fig. 4(f)] phases of the *trans* isomer have the molecules tilted with the hydrophilic head groups on a distorted hexagonal lattice. The domains visible in the BAM images arise from patches of the films containing molecules of different tilt azimuths. The domains within the NNN phase are observed to form more regular structures with more distinct boundaries. The more diffuse boundaries of the NN phase are interpreted to reflect a lower line tension between the domains in this phase. During the NN-to-NNN transition [Figs. 4(b)–4(e)] the contrast between the domains continually increases and evolves due to the 90° difference between the NN and NNN tilt directions. Later, we will discuss the different hydrodynamic responses in both phases under flow.

Figure 5 shows the change of morphology in monolayers transformed using UV irradiation. During photoisomerization the domain boundaries become obscured until a structureless, homogeneous surface is produced. According to the BAM images, a *trans-cis* photoisomerization is induced in each domain, irrespective of the direction of the transition

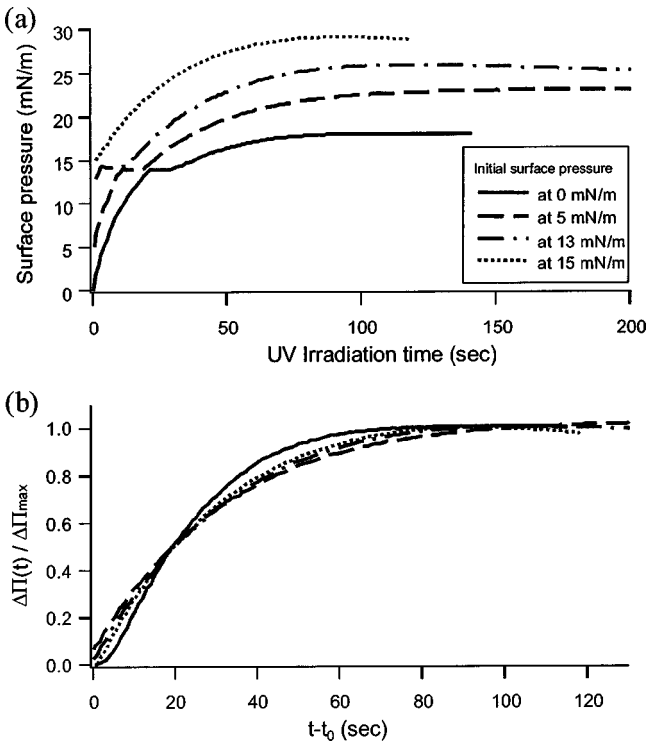

FIG. 6. The kinetics of photoisomerization: (a) The change in surface pressure at a constant surface area with a series of different initial surface pressures; (b) Initial surface pressure dependence of the normalized surface pressure increase versus normalized time calculated by the equation $\Delta\Pi(t)=\Delta\Pi_{\max}(1-e^{-k(t-t_0)})$.

moments of the chromophores under unpolarized UV irradiation. Within the limit of the spatial resolution of the BAM no evidence of phase separation was detected for the *cis* configuration.

C. Kinetics of isomerization

The kinetics of photoisomerization of C_8AzC_3 was studied by measuring the time dependence of the surface pressure during the *trans*-to-*cis* isomerization by UV light of 365 nm at different initial surface pressures, and these results are shown in Fig. 6(a). The increase in surface pressure is due to the fact that isomerization is performed at constant surface area. The surface pressure increases immediately after UV irradiation and reaches the asymptotic value over time. The intermediate, flat region corresponds to the phase transition between the NN and NNN phases.

The isomerization of azobenzene moieties is known to follow first order kinetics in a wide variety of media and phases [3,21]. If we assume first order kinetics, we can derive the reaction rate k from the following equation:

$$\Delta\Pi(t)=\Delta\Pi_{\max}(1-e^{-k(t-t_0)}),$$

where $\Delta\Pi_{\max}$ is the maximum increase of surface pressure and t_0 is the starting time in each phase. The surface pressure profiles for the NNN phase shown in Fig. 6(a) are replotted with a rescaled abscissa suggested by the above equation in Fig. 6(b). Excellent agreement is found for the first order

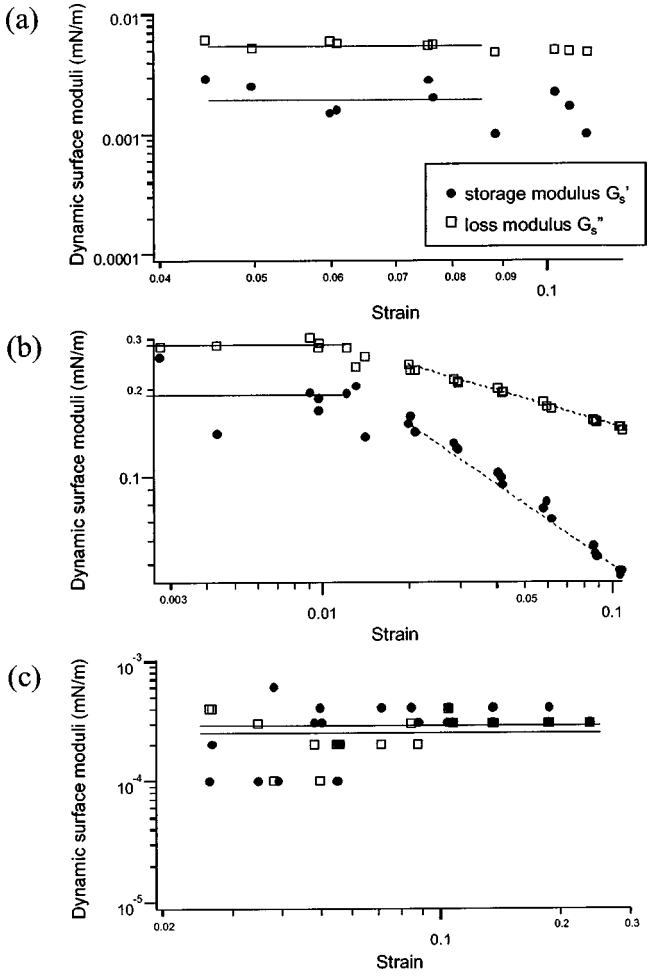

FIG. 7. Surface moduli of C_8AzC_3 monolayers as a function of the strain amplitude: (a) NN phase of *trans* isomer at 11 mN/m; (b) NNN phase of *trans* isomer at 15 mN/m; and (c) *cis* isomer at 15 mN/m. Storage modulus (●) and loss modulus (□).

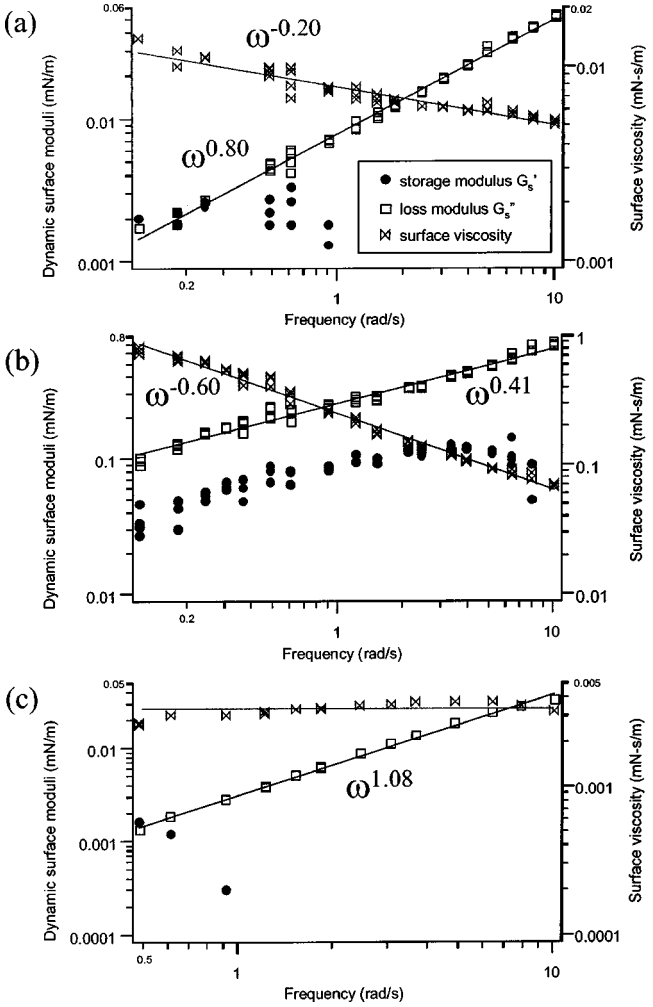

FIG. 8. Surface moduli of C_8AzC_3 monolayers as a function of the frequency: (a) NN phase of *trans* isomer at 11 mN/m; (b) NNN phase of *trans* isomer at 15 mN/m; and (c) *cis* isomer at 15 mN/m. Storage modulus (●), loss modulus (□), and surface viscosity (⋈).

kinetics as demonstrated by overlap of the data. The reaction rate k is 9.50×10^{-2} and 3.55×10^{-2} s^{-1} in the NN and NNN phases, respectively. The low reaction rate k in the high-surface-pressure phase (NNN) suggests that the photoisomerization is hindered in densely packed monolayers due to steric restrictions within the monolayers. These results clearly show the strong influence of monolayer packing and structure on the degree of isomerization.

D. Newtonian and non-Newtonian interfaces

The shear rheology for each phase of C_8AzC_3 was studied. The dependence of the surface moduli on strain amplitude is shown in Fig. 7 for (a) *trans* (NN), (b) *trans* (NNN), and (c) *cis* monolayers. In the NN phase of the *trans* isomer [Fig. 7(a)], both the storage and loss moduli remain nearly constant over the broad range of strain amplitude (<0.08), suggesting that *trans* C_8AzC_3 monolayers at low surface pressure are in the linear viscoelastic regime, like aliphatic fatty acids [10]. However, both surface moduli in the NNN phase of the *trans* isomer [Fig. 7(b)] show nonlinear viscoelastic behaviors at strain amplitudes above 0.01. This trend is also found in liquid crystalline polymeric monolayers where strong interactions between neighboring molecules are observed [10]. All experiments were performed below this strain limit to ensure that the measurements were made in the linear viscoelastic regime. The *cis* isomer showed constant surface moduli for all strain amplitudes that were studied [Fig. 7(c)].

Figure 8 shows the frequency dependence of C_8AzC_3 monolayers for the three different phases. For the *trans* isomer [Figs. 8(a) and 8(b)], the surface viscosity decreases linearly as frequency increases in both the NN and NNN phases. This shear thinning is typical, non-Newtonian behavior. The NNN phase displays enhanced frequency dependence of the surface viscosity compared with the NN phase in *trans* monolayers. It is known that the surface loss modulus scales linearly with frequency for an ideal Newtonian-like interface. The loss moduli are linear on log-log scales with powers of 0.80 and 0.41 in the NN and NNN phases, respectively. It has been argued that increasing the level of molecular attractive interactions or entanglement density gives rise to lower values of the exponent [22,23]. These

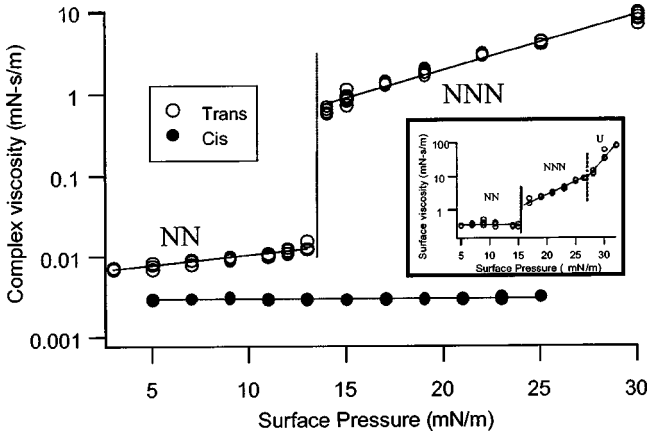

FIG. 9. The surface viscosity for C_8AzC_3 as a function of surface pressure. The surface viscosity undergoes a large increase at a surface pressure of 13.4 mN/m where the phase transition from NN to NNN occurs for the *trans* isomer. The inset figure shows the results for docosanoic acid at 15 °C.

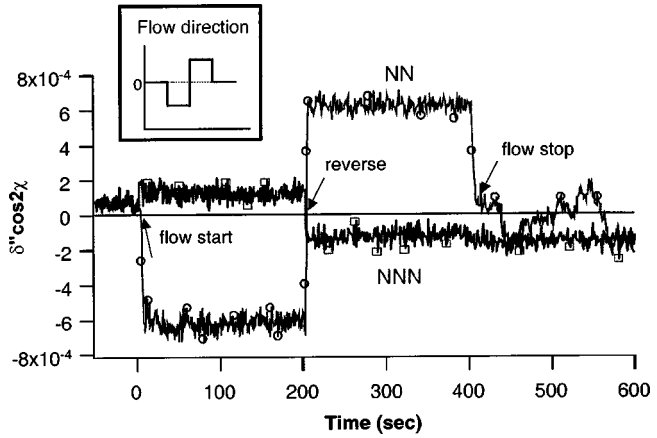

FIG. 10. Orientational response of C_8AzC_3 monolayers of the *trans* isomer to an extensional flow: (○) NN phase at 10 mN/m and (□) NNN phase at 15 mN/m. Inset figure shows the flow direction provided by the four-roll mill.

findings indicate that the NNN phase is more strongly non-Newtonian compared with the NN phase and also possesses a significantly higher storage modulus.

On the other hand, monolayers of the *cis* phase were found to be Newtonian with a constant surface viscosity and a loss modulus that scales linearly with frequency [Fig. 8(c)]. The magnitude of the surface viscosity decreased by a factor of 100 during the *trans*-to-*cis* photoisomerization. It has also been reported that the solution viscosity decreases during *trans*-to-*cis* isomerization for bulk solutions, but the level of decrease is not as much as is found in two dimensions [24]. Clearly, the surface viscosity of monolayers is a very sensitive parameter of molecular structure compared with its use in the bulk, and this is a reflection of the higher degree of order for two-dimensional systems.

E. Thermodynamic transition and its response to shear

Mechanical interfacial rheometry measurements have been performed to obtain an understanding of the relationship between the thermodynamic transition and the response to shear. The logarithm of the surface viscosity is a linear function of the surface pressure based on the two-dimensional theory of reaction rates [25], and the slope and *y*-axis intercept will depend on the particular thermodynamic phase of Langmuir monolayers [10].

The surface viscosities of the *cis* and *trans* states are shown plotted against surface pressure in Fig. 9. The *cis* monolayer was found to have a lower surface viscosity and was Newtonian. The *trans* monolayers, on the other hand, were viscoelastic and underwent a two-order-of-magnitude increase in surface viscosity at a surface pressure of 13.4 mN/m where the phase transition occurs. This increase is substantially larger than the factor of 10 found for docosanoic acid across its phase transition (see the inset in Fig. 9). This difference in the strength of the transition corresponds to the result observed using isotherm data (Fig. 3).

The interaction energy of these rodlike molecules is dominated by long-range van der Waals attractions between hydrocarbon chains and their short-range repulsion. Since the cross section of the azobenzene moiety is larger than that of the alkane chain, it is more difficult for C_8AzC_3 molecules to be sufficiently close for strong attractive interactions compared with aliphatic fatty acids. The significantly smaller surface viscosity of C_8AzC_3 monolayers at low surface pressure (the NN phase) can be explained by this conformational limitation. This is also supported by x-ray diffraction data [18] showing that the in-plane bond length of C_8AzC_3 monolayers in the NN phase is much higher than that of aliphatic fatty acid monolayers, while the bond lengths of both monolayers are comparable in the high-surface-pressure (NNN) phase.

It is known that increasing the alkyl chain length enhances the intermolecular van der Waals interaction, which increases the surface viscosity of the monolayer [26]. In addition, densely packed azobenzene moieties can have π stacking forces, which lead to attractive interactions when aromatic rings are face to face. These forces act in unison to induce high surface viscosities at high surface pressure (the NNN phase) in a manner that is similar to a long-chain fatty acid (C_{22}) in spite of its short tail group (C_8).

Cis monolayers show no transition in the surface viscosity in accordance with the featureless isotherm (Fig. 3), and very low surface viscosity. This suggests that there are no significant molecular interactions between molecules in *cis* monolayers.

On the other hand, a tilting transition between L_2' (NNN) and *S* (untilted) phases in docosanoic acid monolayers results in a continuous transition in the surface viscosity, which reflects its second order behavior observed by isotherms and x-ray diffraction data [27,28]. This clearly implies that there is a close correlation between the thermodynamic phase transition and the macroscopic mechanical shear properties.

F. Comparison of the orientational dynamics

The UV dichroism measurements indicate that the *trans* isomer of C_8AzC_3 monolayers are subject to flow-induced optical anisotropy, while the *cis* isomer forms an isotropic

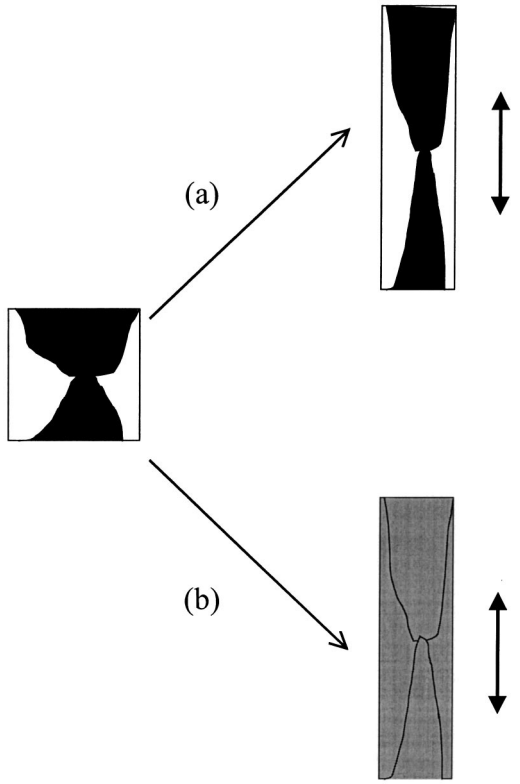

FIG. 11. Schematic representations of a monolayer in (a) NN and (b) NNN phase subject to a flow. Arrows indicate the flow direction.

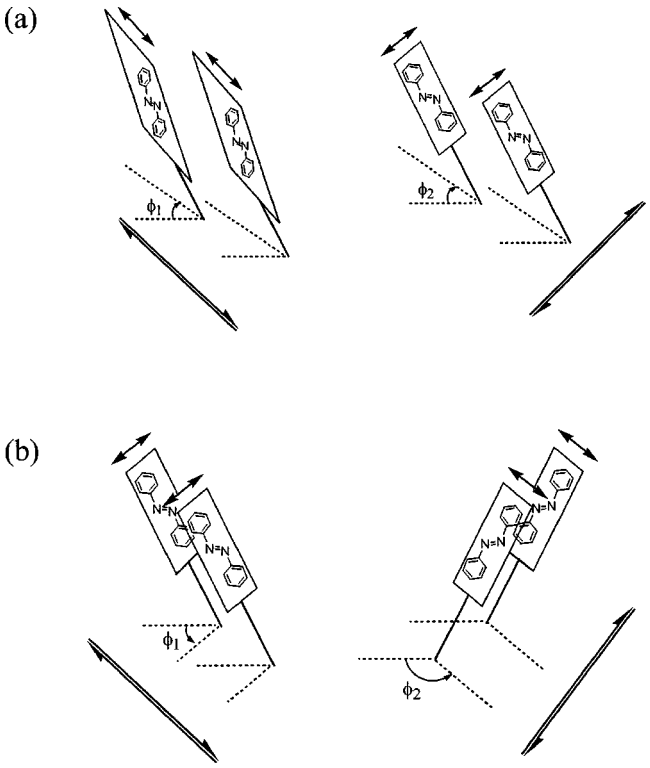

FIG. 12. A molecular packing model for C_8AzC_3 monolayers subject to flow. The single arrows indicate the direction of optical anisotropy measured by dichroism. The double arrows refer to the direction of the flow field. (a) NN phase: The optical anisotropy is parallel to the flow direction. The tilt azimuth is independent of the flow field. (b) NNN phase: The optical anisotropy is perpendicular to the flow direction. The tilt azimuth is coupled to the flow direction.

phase that cannot be oriented using hydrodynamic forces. It is also interesting to compare the orientational dynamics between the NN and NNN phases of the *trans* isomer because the two phases in the *trans* isomer have different crystal lattice structures.

The flow-induced orientation of the *trans* monolayers is shown in Fig. 10 for flow reversal experiments using the four-roll mill. In this figure the extinction δ'' has been multiplied by $\cos 2\chi$ where χ is the average orientation angle of the azobenzene groups and is defined in Fig. 1. By symmetry this angle can either be 0° or 90° and $\cos 2\chi$ is plus or minus unity. The flow reversal protocol used in these experiments first applies a flow with an extension axis that is horizontal for a time of 200 s, after which the flow is reversed to place the extension axis vertical for another 200 s. At 400 s the flow is arrested, and the system is allowed to relax.

The *cis* state could not be oriented by the flows generated by the four-roll mill but a strong dichroism signal was observed for the *trans* state. However, the NN and NNN phases produced qualitatively different responses. First, the azobenzene in the NN phase is unoriented both before inception and following cessation of the flow. This is in contrast to the NNN phase, where this group is oriented at rest. This suggests a nematic response for the NNN phase [29,30]. The second difference is that the dichroism signals for these two phases are of opposite signs, indicating that the same flow orients the azobenzene groups in orthogonal directions. In the NN phase the azobenzene groups are aligned with their short axes parallel to the flow, while the azobenzene moieties in the NNN phase orient with their short axes perpendicular to the stretching direction of the flow.

From the above result of optical anisotropy under flow, it is clear that different microstructure phases show different responses to a flow field. In our previous study [31] using BAM to visualize the morphology of docosanoic acid monolayers under flow, it was found that domains in the NN phase did not change their relative contrast during flow reversal experiments using a four-roll mill. This indicates that the tilt azimuth is unaffected by flow for the NN phase of that fatty acid. However, the NNN phase of docosanoic acid was observed to become aligned by flow, resulting in a change in the relative contrast between domains. The schematic representations of domains subject to flow fields are given in Fig. 11(a) for the NN phase and Fig. 11(b) for the NNN phase.

G. Molecular model of microstructures

The orientation dynamics observed for C_8AzC_3 using UV dichroism and BAM suggests the molecular model of microstructure of this molecule shown in Fig. 12. In the NN phase, the molecules are spaced sufficiently far apart to allow them to rotate freely at a constant tilt azimuth. In the presence of flow, the short axis of the molecules is aligned in the flow direction in order to minimize hydrodynamic resistance. As

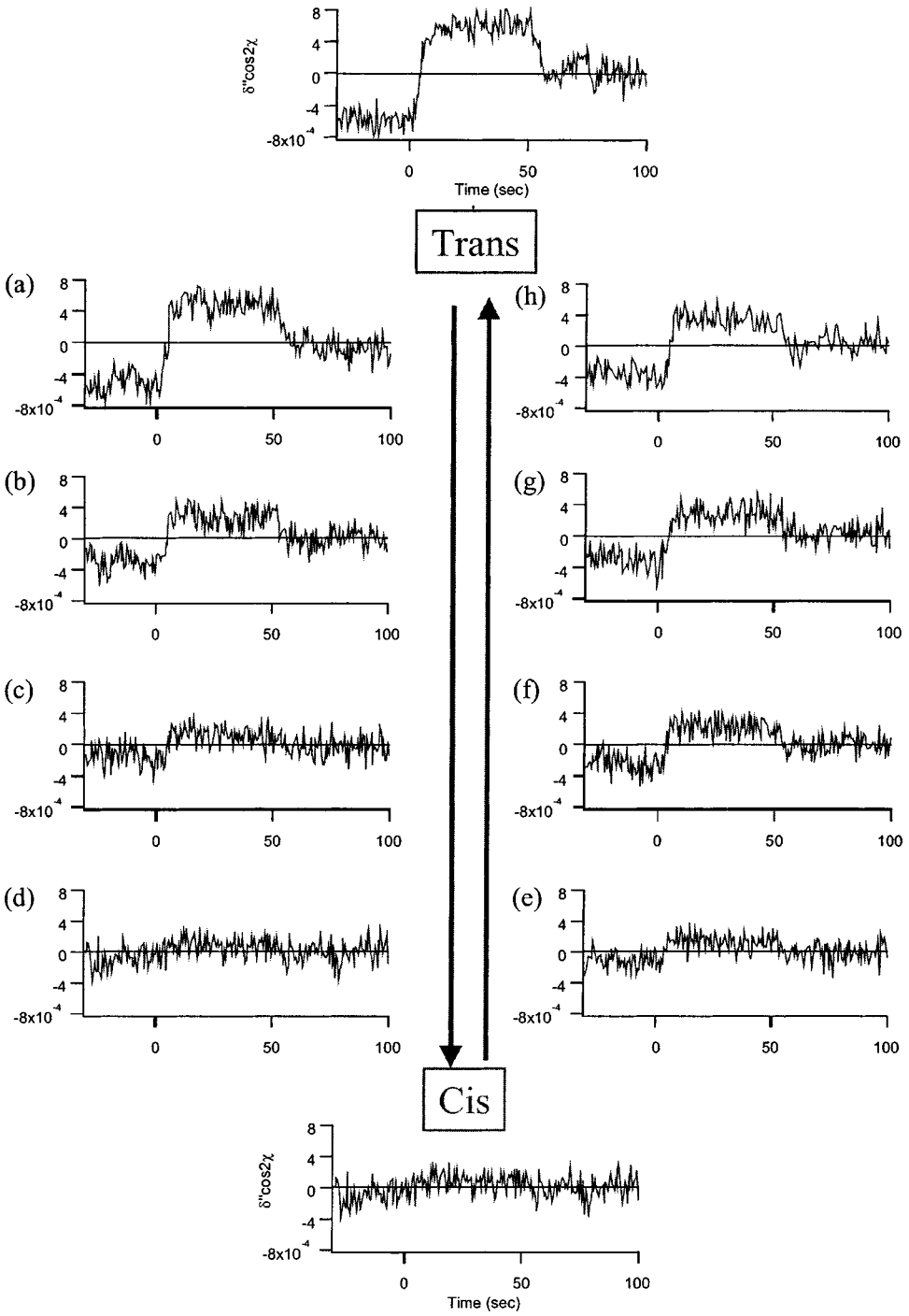

FIG. 13. Effect of photoisomerization on orientation dynamics at 10 mN/m under flow. Top: *trans* isomer; bottom: *cis* isomer. (a)–(d) *trans*→*cis* transition by UV irradiation (365 nm) of (a) 20, (b) 40, (c) 80, and (d) 100 s. (e)–(h) *cis*→*trans* transition by visible light illumination of (e) 2, (f) 8, (g) 12, and (h) 20 min.

shown in Fig. 12(a), the short axis is parallel to the flow direction and the tilted azimuth is independent of the flow field, which agrees with the results of the dichroism measurements and the intensity contrast between crystalline domains subjected to flow as measured using BAM.

In the NNN phase, however, the molecules are packed more densely and this forces the aromatic rings of azobenzene groups to stack ''face to face.'' The dense packing and the resulting strong attractive interactions between adjacent molecules limit the rotation of the azobenzene moiety about its long axis. As a result, the tilt azimuth of molecules in the NNN phase reorients in the flow direction so that the molecules keep their planarity rather than sliding over one another. As pictured in Fig. 12(b), the tilted direction of molecules in the NNN phase is strongly coupled to the applied flow field, and the short axis of the azobenzene molecule is perpendicular to the flow direction. Distorted domain patterns of the NNN phase generated by flow do not appear to relax in shape but remain stable in appearance once the flow is stopped, which agrees with the finding of a nematic phase observed using dichroism (Fig. 10).

A recent study [18] using x-ray diffraction on C_8AzC_3 monolayers reported that the bond lengths in the horizontal plane jump down below the width of the azobenzene moiety

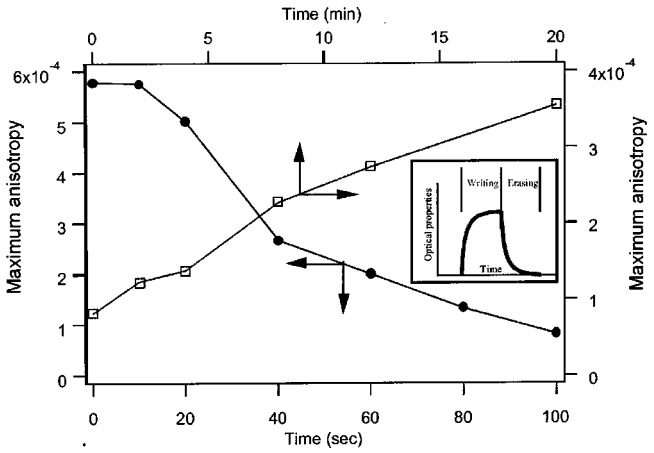

FIG. 14. Change in optical anisotropy as photoisomerization proceeds at 10 mN/m. *trans*→*cis* transition by UV light (●) and *cis*→*trans* transition by visible light (□). Inset is the schematic representation of a typical writing-erasing process for optical data storage.

dramatically at the NN-to-NNN transition, supporting our molecular packing model as described in Fig. 12. We also performed a study of orientational dynamics in mixtures of C_8AzC_3 monolayers with amphiphilic molecules such as stearic acid. Interestingly, the addition of stearic acid leads to the absence of a phase transition in *trans*-C_8AzC_3 monolayers. In these mixed monolayers, the azobenzene groups orient parallel to the flow even at a high surface pressure of 20 mN/m (data not shown). This is due to the fact that mixtures of C_8AzC_3 and stearic acid intercalate and enlarge the distance between adjacent C_8AzC_3 molecules, thereby inhibiting close packed structures.

The relative tilt and orientation of the azobenzene moiety in monolayers are not clearly known at this moment due to the lack of a study on the crystal structures associated with these systems. However, our molecular model in this study gives a reasonable picture of molecular packing and explains the complicated orientational dynamics and the contrast change of BAM images under the flow.

H. Photoinduced anisotropic-to-isotropic phase transition

A systematic study of the effect of photoisomerization on molecular anisotropy and the orientational dynamics of C_8AzC_3 monolayers was carried out at 10 mN/m (the NN phase) using UV dichroism. Results of this experiment are shown in Fig. 13. Each graph in this figure plots $\delta'' \cos 2\chi$ against time during flow reversal experiments. We have the results for the NN phase of the *trans* state (topmost graph) down to the *cis* state (lowermost graph). As expected, the evolution from the *trans* to the *cis* state by the application of UV irradiation is accompanied by a reduction in the degree of flow-induced orientation. Indeed, the *cis* state remains isotropic under flow. This is a reversible phenomenon, and applying visible light to the monolayers reverts the molecules back to the *trans* form [Figs. 13(e)–13(h)].

This transition from anisotropic to isotropic states is related to the modification of molecular structure at the air/water interface during photoisomerization. The linear rodlike structure in the *trans* isomer enables molecules to align into the preferred tilted direction, resulting in anisotropic domains. This anisotropy vanishes as the *trans* isomer begins to transform into a bent-shaped *cis* isomer that cannot form regularly ordered structures.

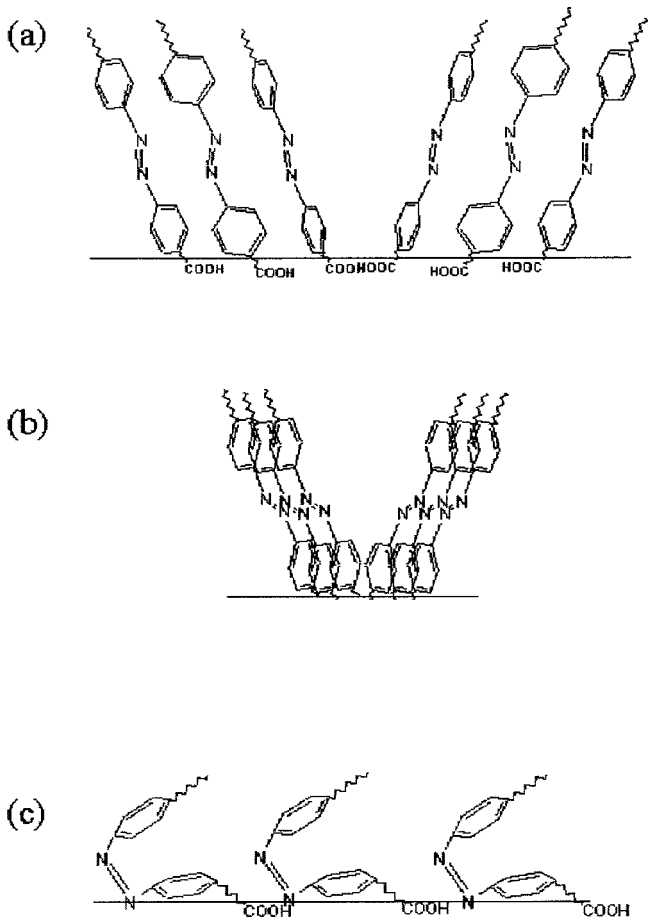

FIG. 15. Schematic representations of packing structures of monolayer molecules in (a) NN and (b) NNN phase in *trans* isomer and (c) *cis* isomer.

Figure 14 shows the dependence of maximum anisotropy on the light illumination time. The maximum anisotropy begins to decrease as photoisomerization by UV light proceeds, and it rises as visible light is illuminated. The scale of the axes in the two processes is different because the intensities of UV and visible light are not normalized.

An interesting application based on photoisomerization concerns optical storage systems. Azobenzene-containing materials are good candidate materials for optical recording media due to their high optical sensitivity, short switching and access times, and reversibility after many write-erase cycles [32,33]. The monolayer molecules at the air/water interface can be easily transferred onto a solid substrate using Langmuir-Blodgett deposition, during which the molecular orientation and packing are controlled. Figure 14 shows a sharp transition in the optical anisotropy of a monolayer that mimics a typical write-erase process in an ultrathin film device (see inset in Fig. 14).

IV. SUMMARY

We investigated the thermodynamic phase transition and the surface rheological properties of an azobenzene-containing fatty acid C_8AzC_3 monolayer. This material is particularly interesting because it shows anisotropic orientational dynamics as well as a well-ordered thermodynamic phase diagram, which can be examined by UV polarimetry and BAM, respectively.

It was found by isotherm measurements that a strong first order transition exists between the NN and NNN phases in the *trans* isomer, which was revealed using BAM. At this transition, the magnitude of the surface viscosity was increased by a factor of about 100. In the low-surface-pressure, NN, phase, monolayer molecules are far enough from each other due to bulky azobenzene moieties to reduce the attractive interaction and surface viscosity. The molecule can rotate freely along the long axis of azobenzene, allowing the short axis to align toward a flow field as described in Fig. 12(a). After the flow stops, the molecules rotate to relax and return to the random isotropic phase.

On the other hand, at high surface pressure (the NNN phase), azobenzene moieties in a dense packing can have π stacking forces in a face-to-face arrangement of aromatic rings, which leads to the formation of a nematic phase. The strong attractive interaction causes the monolayer molecules to reorient parallel to the flow direction to keep their planarity, resulting in the direction of the short axis of the azobenzene moiety being perpendicular to the flow field [Fig. 12(b)].

Photoisomerization by UV or visible light caused dramatic changes in both thermodynamic and rheological properties. The UV light of 365 nm induced isomerization from the *trans* to the *cis* isomer and changed molecular structures from linear- to bent-shaped forms. As a result, molecules occupy a higher surface area and the phase transition disappears. This is due to the fact that bent shapes and polar properties in the *cis* isomer drive molecules to have irregular and random structures without specific molecular interactions. This was confirmed by homogeneous BAM images and the absence of anisotropic phenomena under flow for the *cis* state. Figure 15 gives the schematic representation of each phase at the air/water interface.

From this study, the correlation between thermodynamic phases and their different rheological responses in two-dimensional monolayers was obtained by several experimental techniques and a molecular model accounting for these observations has been proposed.

ACKNOWLEDGMENTS

The authors thank Dr. M. K. Durbin and Dr. P. Dutta at Northwestern University for useful discussions. The authors also acknowledge support from the NSF-CTS Division and partial support from the Center on Polymer Interfaces and Macromolecular Assemblies (a NSF-MRSEC).

[1] B. L. Feringa, R. A. vanDelden, N. Koumura, and E. M. Geertsema, Chem. Rev. **100**, 1789 (2000).
[2] G. S. Kumar and D. C. Neckers, Chem. Rev. **89**, 1915 (1989).
[3] S. Xie, A. Natansohn, and P. Rochon, Chem. Mater. **5**, 403 (1993).
[4] T. Ikeda and O. Tsutsumi, Science **268**, 1873 (1995).
[5] Y. Tabe and H. Yokoyama, Mol. Cryst. Liq. Cryst. Sci. Technol., Sect. A **358**, 125 (2001).
[6] J. J. DeLang, J. M. Robertson, and I. Woodward, Proc. R. Soc. London, Ser. A **171**, 398 (1939).
[7] V. M. Kaganer, H. Mohwald, and P. Dutta, Rev. Mod. Phys. **71**, 779 (1999).
[8] M. C. Friedenberg, G. G. Fuller, C. W. Frank, and C. R. Robertson, Macromolecules **29**, 705 (1996).
[9] K. S. Yim *et al.*, Langmuir **16**, 4319 (2000).
[10] K. S. Yim *et al.*, Langmuir **16**, 4325 (2000).
[11] G. G. Fuller, Annu. Rev. Fluid Mech. **22**, 387 (1990).
[12] J. J. L. Higdon, Phys. Fluids A **5**, 274 (1993).
[13] C. F. Brooks, G. G. Fuller, C. W. Frank, and C. R. Robertson, Langmuir **15**, 2450 (1999).
[14] D. L. Beveridge and H. H. Jaffe, J. Am. Chem. Soc. **88**, 1948 (1966).
[15] R. Ionov and A. Angelova, J. Phys. Chem. **99**, 17 606 (1995).
[16] M. Matsumoto *et al.*, Langmuir **11**, 660 (1995).
[17] Z. J. Zhang *et al.*, Langmuir **13**, 4422 (1997).
[18] M. K. Durbin *et al.*, Langmuir **14**, 899 (1998).
[19] H. Nakahara and K. Fukuda, J. Colloid Interface Sci. **93**, 530 (1983).
[20] T. Kawai, J. Umemura, and T. Takenaka, Langmuir **5**, 1378 (1989).
[21] Z. F. Liu *et al.*, J. Phys. Chem. **96**, 1875 (1992).
[22] A. Koike, N. Nemoto, M. Takahashi, and K. Osaki, Polymer **35**, 3005 (1994).
[23] C. Iversen *et al.*, Polym. Bull. (Berlin) **39**, 747 (1997).
[24] M. Irie, Y. Hirano, S. Hashimoto, and K. Hayashi, Macromolecules **14**, 262 (1981).
[25] W. J. J. Moore and H. Eyring, J. Chem. Phys. **6**, 391 (1938).
[26] H. Huhnerfuss, J. Colloid Interface Sci. **107**, 84 (1985).
[27] S. Stallberg-Stenhagen and E. Stenhagen, Nature (London) **156**, 239 (1945).
[28] V. M. Kaganer *et al.*, J. Chem. Phys. **102**, 9412 (1995).
[29] R. M. Kenn *et al.*, J. Phys. Chem. **95**, 2092 (1991).
[30] The ordered phases of monolayers are often compared to smectic phases of liquid crystals. However, only orientational order is measured in this study and the authors favor use of the term ''nematic.''
[31] T. Maruyama, G. Fuller, C. Frank, and C. Robertson, Science **274**, 233 (1996).
[32] K. Anderle, R. Birenheide, M. J. A. Werner, and J. H. Wendorff, Liq. Cryst. **9**, 691 (1991).
[33] R. Piron, E. Toussaere, D. Josse, and J. Zyss, Appl. Phys. Lett. **77**, 2461 (2000).